Orientational Dynamics in the Isotropic Phase of a Calamitic Liquid-Crystal Model

Davide Bertolini[†]

Istituto per i Processi Chimico-Fisici, CNR, Via G. Moruzzi 1, I-56124 Pisa, Italy

Giorgio Cinacchi,* Luca De Gaetani,[‡] **and Alessandro Tani**[§]

Dipartimento di Chimica, Università di Pisa, Via Risorgimento 35, I-56126, Pisa, Italy

Received: June 20, 2005; In Final Form: October 17, 2005

We report a molecular dynamics simulation study on the isotropic phase of an idealized calamitic liquid crystal model with a length-to-width ratio of ≃5−6. The study focuses on the characterization of single-particle and collective orientational dynamics on approaching the phase transition to the nematic phase. Recent experimental and simulation works have suggested that a power law behavior exists at relatively short times in the decay of the time derivative of the orientational correlation functions. Qualitatively, our simulation data are consistent with these findings. Both single-particle and collective time correlation function derivatives possess, in their respective log−log plots, a linear region at very short times, whose slope is essentially independent from the thermodynamic state. Nevertheless, the single-particle orientational correlation functions are better described by a function which is the sum of a fast exponential, an intermediate stretched-exponential and a slow exponential, while the collective orientational correlation functions are satisfactorily described by a sum of two exponentials, at higher density, or by just one exponential, at lower density.

1. Introduction

The isotropic (I) to nematic (N) phase transition is experimentally known to be weakly first order.[1,2] It has appeared natural to believe that the short-range structure of nematogenic fluids changes smoothly across the above-mentioned phase transition. This approximation, at the heart of the Lebwohl−Lasher (LL) lattice model[3] and its variants,[4] has received a recent clear confirmation by the calculation of the direct correlation function (DCF) in a system of modified Gay−Berne (GB) particles: in fact, the DCF was found to remain short-ranged and weakly affected by the approach to the IN phase transition (INPT).[5] The LL model, originally devised to test Maier−Saupe mean field theory for nematics,[6] was later demonstrated to provide a good account of the peculiarities of the INPT, including the presence of pretransitional phenomena.[7,8] The latter, observed experimentally, are a consequence of the weak character of the IN phase transition and were predicted by De Gennes, who extended the Landau theory of second-order phase transitions to the INPT.[1]

According to Landau−De Gennes (LDG) theory, the isotropic phase of a nematogenic fluid is seen as composed of pseudonematic domains, whose characteristic dimension, $l(T)$, grows with decreasing temperature as follows:

$$l(T) = l_0\left[\frac{T^*}{T - T^*}\right]^{1/2} \tag{1}$$

where l_0 is approximately the molecular length, and T^* a temperature usually ∼1−2 K lower than T_{IN}, the temperature at which the INPT occurs. LDG theory predicts, in addition, that the orientation of the pseudonematic domains relaxes exponentially with a characteristic time given by

$$\tau_{LDG} \propto \frac{\eta(T)}{(T - T^*)} \tag{2}$$

where $\eta(T)$ is the shear viscosity. Equations 1 and 2 have received several experimental confirmations (see refs 9−11 and references therein), provided T is not too far from T^*. Slightly above T^*, pseudonematic domains are present, and relatively large and long-lived; on increasing temperature, their dimensions become progressively smaller, and it is natural to believe that they form, disrupt and reform with an increasingly larger frequency. At sufficiently large temperatures, l is comparable to the molecular dimensions: the domains no longer exist and the orientation of a molecule should relax according to the Debye law:

$$\tau_{DEB} \propto \frac{\eta(T)}{T} \tag{3}$$

The structure and interdomain orientational dynamics in the isotropic phase of a nematogenic fluid approaching the INPT are reasonably well understood. The interest in the intradomain dynamics has been recently renewed by the experiments described in refs 9−14, all seemingly indicating the existence of a temporal power law in the short-time decay of the optical Kerr effect (OKE) experimental signal. The latter should be essentially proportional to the time derivative of the collective orientational correlation function. Early experiments were believed indicative of an universal value of the exponent of the power law component, equal to −0.63;[9−11] a theory was then developed to account for this behavior.[15] Later experiments,[12−14] however, have suggested that the exponent should be related to the effective length-to-width ratio (κ) of the nematogenic

* E-mail: g.cinacchi@sns.it.
† E-mail: davide@ipcf.cnr.it.
‡ E-mail: degaetani@dcci.unipi.it.
§ E-mail: tani@dcci.unipi.it.

10.1021/jp0533067 CCC: $30.25
Published on Web 12/03/2005

Figure 1. Calamitic liquid-crystal model adopted.

molecules. The new theoretical analysis[12] has led to an expression of the collective orientational correlation function valid for intermediate times, and such that its derivative decays as a power law in an appropriate short-time limit.

The relaxation of single-particle and collective orientational correlation functions has been also the subject of a few computer simulation studies.[5,16−19] Computer simulations are a very valuable tool that provides an effective bridge between theory and experiments, particularly when performed on simplified models. Early computer simulation studies were able to observe a significant slowing down of the collective orientational relaxation near the INPT.[16,17] The decay of both single-particle and collective functions was found to be substantially exponential,[16,17] even though the predictions of the Debye small-step rotational diffusion model deteriorate as density is increased.[17] Particularly interesting are the results of ref 5, since they anticipate, at a qualitative level, the essence of later experimental outcomes: the decay of the Fourier transform of the collective orientational correlation function was found to be exponential for not too large wavenumber, and the approach to the INPT affects only the longest wavelength dynamical properties. Power law decay in the single-particle second rank orientational correlation functions was observed in refs 18 and 19, where also second rank collective orientational correlation functions have been calculated. The power law component seems to emerge in the close vicinity of the INPT for both single-particle and collective functions.

All numerical studies performed so far have adopted uniaxial ellipsoids, either hard or of the GB type, and with $\kappa \leq 3$, as models for the nematogenic molecules. However, it is known that shape has a profound influence on liquid-crystalline properties.[20] Therefore, we have thought it worthwhile to extend the above-mentioned calculations to another calamitic liquid-crystal model, namely an array of nine soft spheres arranged linearly so that the overall particle resembles a spherocylinder of $\kappa \simeq 5-6$. In refs 21 and 22, the phase behavior, structure, diffusion and viscosity of an ensemble of 600 such particles have been recently investigated. The present work focuses on the orientational dynamics of the same system in the isotropic phase. Molecular dynamics (MD) simulations in the microcanonical (NVE) statistical ensemble have been performed close to the INPT. Details about these calculations are provided in the next section, while the results are presented and discussed in section IV. Conclusions are finally drawn in section V.

2. Details on Model, Molecular Dynamics Simulations, and Computed Quantities

The mesogenic particles considered are depicted in Figure 1. They are formed by nine soft spherical beads, held rigidly on a line. Contiguous beads are kept at a distance of 2.34 Å, while any pair of sites belonging to different particles interact according to the reference soft repulsive potential in the Weeks-Chandler-Andersen separation of the Lennard-Jones potential, with $\sigma_0 = 3.9$ Å and $\epsilon_0 = 6 \times 10^{-22}$ J.[21,22] Only the two extreme sites bear a mass $m = 15 \times 1.67 \times 10^{-24}$ g.[22]

MD-NVE simulations (see ref 22 for a discussion on why the microcanonical ensemble has to be used if the interest is in calculating dynamical quantities) on a system of such rods, with $N = 600$, have been performed at the state points in the isotropic phase reported in Table 1. The equation of motions have been integrated by the Verlet algorithm with a time-step of 5 fs and the method of constraints has been employed to keep the particle linear and the constituent beads at the pre-selected distance (see the appropriate references cited in refs 21 and 22).

TABLE 1: Thermodynamic Properties of the Four State Points Investigated

state point	pressure (kbar)	temperature (K)	density (1000 Å^{-3})
I	2.48	598	2.076
II	2.56	623	2.070
III	2.57	636	2.053
IV	2.51	632	2.040

In the present work, the interest is in the calculation of second-rank single-particle and collective orientational correlation functions. They are, respectively, defined as

$$C_2^{s}(t) = \langle P_2(\hat{\mathbf{u}}_i(t)\cdot\hat{\mathbf{u}}_i(0))\rangle \tag{4}$$

and

$$C_2^{c}(t) = \sum_{j=1}^{N}\langle P_2[\hat{\mathbf{u}}_j(t)\cdot\hat{\mathbf{u}}_i(0))\rangle \tag{5}$$

where $\langle\rangle$ mean an average over particles i and time origins, P_2-() is the second-rank Legendre polynomial, and $\hat{\mathbf{u}}_i(t)$ is the unit vector defining the orientation of particle i at time t. Since the calculation of any collective quantities requires quite long runs to accumulate averages with an acceptable statistics, the production runs lasted 20 ns at least, after a 1 ns run of equilibration in an isothermal−isobaric ensemble (see the appropriate references cited in refs 21 and 22). This length of the production runs results in a reasonable compromise between accuracy of the collective functions and computational effort.

3. Results and Discussion

The signal detected in the OKE experiments should be essentially proportional to $\dot{C}_2^{c}(t)$, the time derivative of the collective orientational correlation function defined in eq 2. The experiments described in refs 9−14 span a time window approximately between 1 ps to 100 ns. The signal of the most recent experiments[12−14] has been successfully fitted over the entire time window with the following function:

$$f(t) = \mathrm{e}^{-t/\tau_{LDG}}[a + \mathrm{e}^{-t/\gamma}(b + ct^{-p})] \tag{6}$$

The first exponential term describes the decay at long times (e.g., >1 ns for real substances). This relaxation is governed by the quantity τ_{LDG}, that is given by eq 2. This term is thought to describe the relaxation of pseudonematic domains that exist in the isotropic phase of a nematogenic fluid in the vicinity of the INPT. The terms in the square brackets, instead, are supposed to account for the intradomain relaxation, occurring on a shorter time scale (e.g., >1 ps and <1 ns for real substances).

Typical experimental values for the parameters entering eq 6 are as follows: $\tau_{LDG} \sim 50$ ns; $a \sim 1$; $\gamma \sim 10$ ns; $b \sim 0.1$; $c \sim 0.13$; $p \sim 0.65$.[12−14] Figure 2 shows the $f(t)$ function obtained with these parameters together with the separated contribution of the biexponential term

$$B(t) = \mathrm{e}^{-t/\tau_{LDG}}[a + b\mathrm{e}^{-t/\gamma}] \tag{7}$$

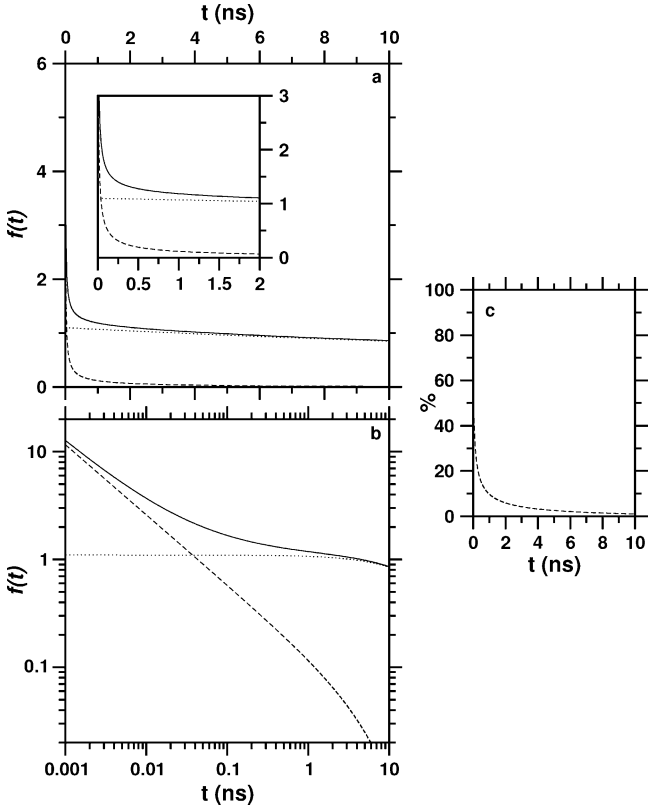

Figure 2. Typical curve of the optical Kerr effect experimental signal. (a) The function $f(t)$ (solid line) is plotted together with the biexponential (eq 7, dotted line) and the exponential-power law (eq 8, dashed line) contributions. The inset shows details at short times. (b) The same as in part a but on a log−log scale. (c) The percentage contribution to $f(t)$ of the exponential-power law term (dashed line).

and of the exponential-power law term,

$$P(t) = c\mathrm{e}^{-t/\tau_{\mathrm{LDG}}}\,\mathrm{e}^{-t/\gamma}t^{-\mathrm{p}} \tag{8}$$

It is apparent that $B(t)$ plays the major role at all but the very short times. Even in the time window 1 ps $< t <$ 1 ns, the contribution of $P(t)$ is far from being dominant, and a power law decay stands out clearly in a log−log plot of $P(t)$ for times smaller than ∼100 ps. The decay of $f(t)$ is almost purely of the power-law type only at very short times, smaller than ∼10 ps.

The integration of eq 6 leads to a normalized orientational correlation function of the following form[12]

$$F(t) = \frac{\alpha\mathrm{e}^{-t/\tau_{\mathrm{LDG}}} + \epsilon\mathrm{e}^{-Kt} + \lambda\Gamma(1-p, Kt)}{\alpha + \epsilon + \lambda\Gamma(1-p)} \tag{9}$$

with the set of parameters $\{\alpha,\tau_{\mathrm{LDG}},\epsilon, K, \lambda, p\}$ appropriately related to the corresponding set of parameters entering eq 6, and $\Gamma(1-p, Kt)$ being the incomplete gamma function:

$$\Gamma(1-p, Kt) = \int_{Kt}^{\infty} s^{-p}\mathrm{e}^{-s}\,\mathrm{d}s \tag{10}$$

It is fair to mention at this point that the experimental curves presented in refs 12−14 have been also fitted in a successive paper[23] with a function similar to eq 6, but without the coefficient a and the inner exponential replaced by another power law. The same function was used to fit experimental data for a few supercooled liquids, stressing the analogy between the dynamics in the isotropic phase of a nematogenic liquid and that in a supercooled liquid.[23,24] The latter fitting process did not show, however, any apparent improvement with respect to the former, already successful for the isotropic liquid crystals examined.

Equation 6 is clearly not the only eligible functional form having a power law term. One further candidate is certainly the time derivative of a sum of a stretched exponential and two exponentials, that is the time derivative of the following function:

$$S(t) = q_1\mathrm{e}^{-t/\tau_{\mathrm{LDG}}} + q_2\mathrm{e}^{-(t/v)^{\xi}} + q_3\mathrm{e}^{-t/\delta} \tag{11}$$

The stretched-exponential function has often proven very effective in accounting for a variety of relaxation dynamics phenomana in dense fluid and glassy systems.[25−28] The exponent ξ is equal to unity in the case of a diffusive rotational motion and becomes progressively smaller than 1 as the rotational dynamics becomes more frustrated. The stretched-exponential is a remarkably successful function with an empirical origin,[25] although physical models have been formulated to give it a possible basic interpretation.[27,28] As these theories are always generic and phenomenological in character, we share the position of ref 27, where it is stated that the detailed interpretation of a theory of the stretched-exponential function depends peculiarly on the system to which it is applied. In the present case, the stretched-exponential function, together with the fastest exponential term, are thought to describe the short-time orientational relaxation within a pseudonematic domain. The residual anisotropy then relaxes at longer times through the usual LDG exponential. In view of the possible analogy between orientational relaxation in the isotropic phase of a nematogenic liquid crystal close to the INPT and the relaxation dynamics in supercooled liquids,[23,24,29] it would be interesting to apply eq 11 in the analysis of the experimental data of ref 23.

Equations 9 and 11 have as limiting cases, the biexponential function (eq 7) and its immediate extension, that is a triexponential function:

$$G(t) = \mathrm{e}^{-t/\tau_{\mathrm{LDG}}}[g_1 + \mathrm{e}^{-t/\gamma}(g_2 + g_3\mathrm{e}^{-t/\delta})] \tag{12}$$

The latter have been often proven adequate to describe the experimental signal, obtained in a number of experiments on the dynamics of isotropic liquid crystals, without the necessity to consider a power-law term.[30−34] The term inside the square brackets is again thought to describe the orientational relaxation within one of the pseudonematic domains, the latter then relaxing according to LDG theory. It is of interest to note that, when the data have been reasonably described by a biexponential function,[30,31] it turned out that the faster decay time follows approximately the Debye law, and increases gently with temperature without displaying any pretransitional effect. Conversely, the slower decay time that was shown to follow LDG theory and, therefore, is rapidly growing close to the INPT. With the help of accompanying data on the dynamics of a judiciously chosen probe dissolved in the isotropic phase of the liquid crystals of interest, it was later shown that the dynamics of the latter can be better described by a triexponential function.[32] Besides the long-time LDG exponential relaxation, the dynamics occurring on a shorter time scale could be well described by the remaining two exponential terms. The faster component turned out to be Debye-like, while the characteristic time of the intermediate component displays a more complex behavior, comprised between that emerging from Debye and LDG laws. Debye-like character of the reorientational time is also shown by several solutes dissolved in isotropic liquid crystals.[35,36]

The above considerations have guided our analysis of the single-particle (eq 4) and collective (eq 5) second-rank reori-

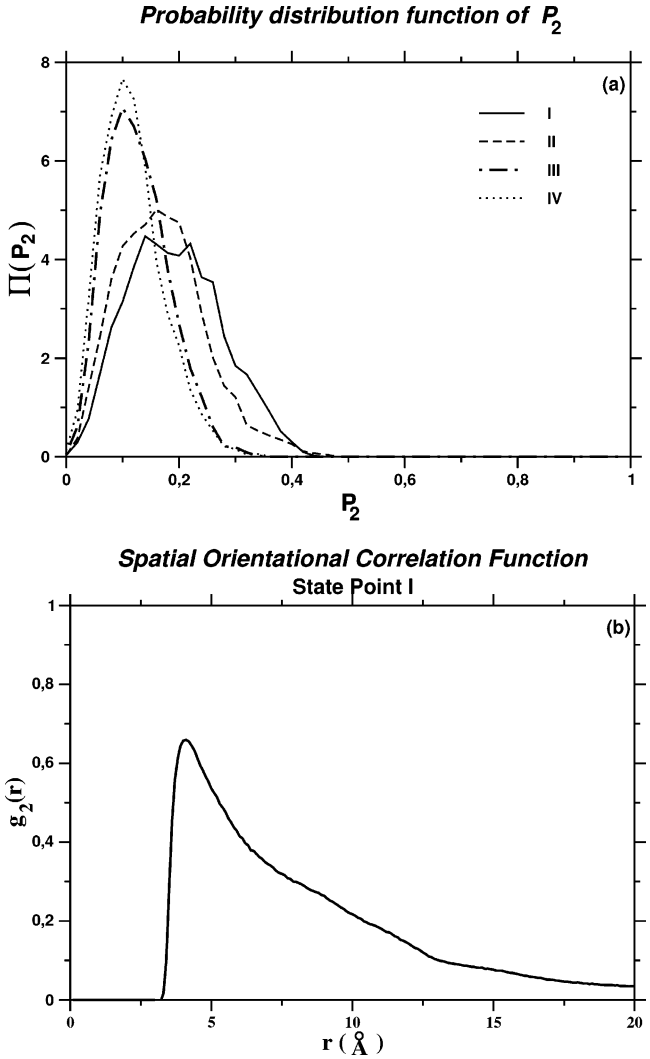

Figure 3. (a) Probability distribution functions of the orientational order parameter, $\Pi(P_2)$, in the four state points investigated; these functions are normalized to 1. (b) Spatial orientational correlation function for state point **I**.

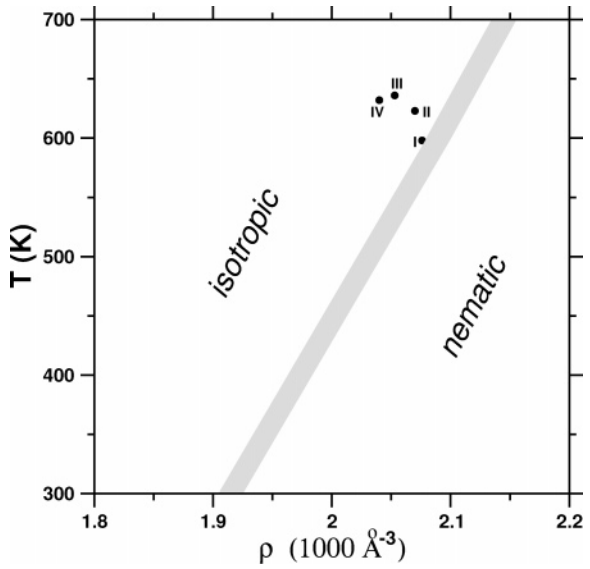

Figure 4. Isotropic−nematic phase diagram of the nine-beadlace model in the density−temperature plane and the four state points investigated.

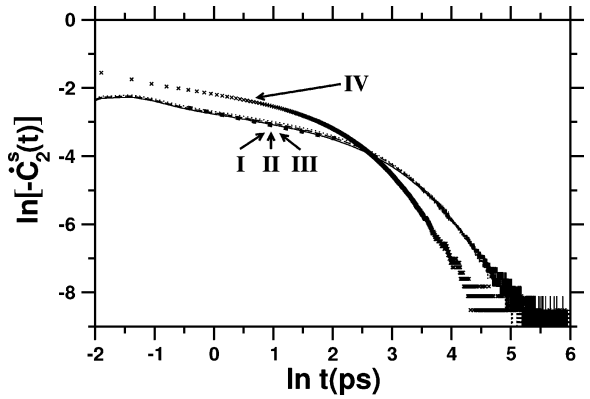

Figure 5. Time derivative of the single-particle orientational correlation functions on a log−log scale. The dotted line is a linear fit with a slope of −0.35.

entational correlation functions calculated for our model particles at the four state points listed in Table 1. State points **II**, **III**, and **IV** can be considered belonging to the isotropic phase of the 9-site model described above, yet close to the transition to the nematic phase (Figure 3a and 4). State point **I** is characterized by an orientational order parameter ≃0.2. The unimodal character of the orientational order parameter distribution function suggests that it should be considered in the isotropic phase, very close to the phase transition boundary (Figure 3a and 4). In Figure 3b the spatial orientational correlation function, $g_2(r)$, for state point **I** is also shown (for its definition, see, e.g., ref 7).

As the model particles adopted are soft repulsive, density is the thermodynamic quantity chosen as the best control parameter of their behavior (Figure 4).

3.1. Single-Particle Orientational Relaxation. The single-particle orientational correlation functions have been evaluated for the time interval 0−1.5 ns and are affected by an error, estimated according to ref 37, of 0.5% at most. First, we have computed $C_2^s(t)$, and then numerically evaluated their time derivative, $\dot{C}_2^s(t)$, employing the centered difference method. In Figure 5 the functions $\dot{C}_2^s(t)$ are reported on a log−log scale. We note that time derivatives at the state points **I**, **II**, and **III** are, at short times, essentially the same, while that of state point **IV** is different. It seems, therefore, that the time derivative of the second rank single-particle orientational correlation functions becomes, at short times, progressively density independent on approaching the INPT. In the time interval $\ln t \in [-0.5;2.0]$, the behavior of $\ln[-\dot{C}_2^s(t)]$ at state points **I**, **II**, and **III** appears reasonably linear and the fit gives a slope of ∼-0.35. This would seem to suggest that in the approximate interval $t \in [0.5;5]$ps a power law decay exists in the time derivative of the single-particle orientational correlation functions in isotropic phase close to the INPT. However, the fitting[38] of $\dot{C}_2^s(t)$ with the empirical function $f(t)$ (eq 6) reveals that the time derivative of the single-particle orientational correlation functions is well described by a biexponential function (eq 7). The term in eq 6 plays no role, being the optimized value of c always equal to 0.

This leads us to conclude that the power law term in eq 2, which is used to fit the time derivatives of the single-particle orientational correlation functions, gives a very minor contribution to the overall RMS.[38]

The straightforward consequence of the biexponential character of $\dot{C}_2^s(t)$ is that also the single-particle orientational correlation functions (Figure 6) can be described by a sum of two exponential terms (eq 7, with $a + b = 1$ in order to ensure that $C_2^s(0)=1$). However, improved fittings are obtained by describing $C_2^s(t)$ with the functions $F(t)$ (eq 9; although this empirical function was actually derived on the basis of the OKE

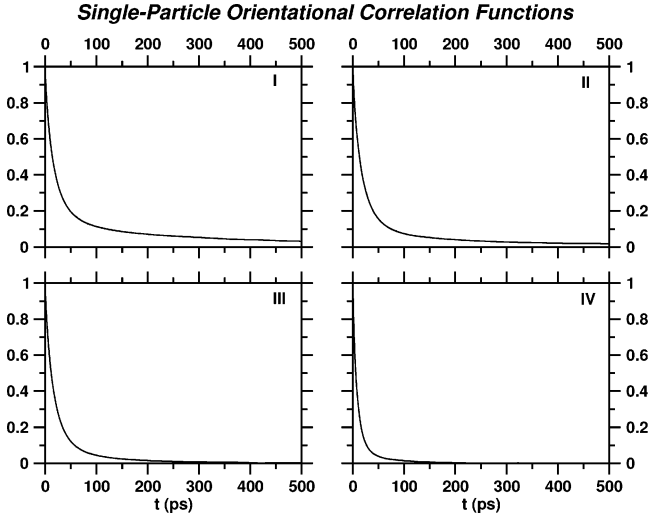

Figure 6. Single-particle orientational correlation functions obtained in simulations. The corresponding functions fitted via eqs 9, 11, and 12 are indistinguishable from the simulation curve on this scale.

experiments, we can adopt it as a general fitting function), $S(t)$ (eq 11) and $G(t)$ (eq 12), all properly normalized. The parameters of these fittings as well as the RMS deviations[38] are reported in Tables 2 (a)−(d) for all the state points indicated with Roman numerals. Basically, all the functional forms investigated provide a good fit, and the slight improvements of eqs 9, 11, and 12 over the biexponential function may be simply due to the increased number of free parameters. It is fair to observe that the best performance is obtained with the function $S(t)$ (eq 11), that is especially good in reproducing both the short-time linear region in the log−log plot of the time derivatives and the long-time tail of the single-particle orientational correlation functions. This can be noticed in Figure 7 for the more delicate case of state point **I**. The function $F(t)$ (eq 9), notwithstanding the largest number of free parameters available, shows the largest RMS's. In addition, the second exponential term in eq 2 seems redundant, being the optimized value of ϵ equal to 0. The triexponential function $G(t)$ (eq 12) gives fits of intermediate quality. However, parts a and c of Figure 7 reveal that the short-time part of the $C_2^s(t)$ and of its time derivative is not well reproduced by the triexponential function.

Irrespective of the functional form used to describe the numerical data, a general trend can be noticed: moving toward the INPT, the LDG exponent tends to grow significantly while the characteristic time of the faster relaxation terms has a less pronounced increment. This has to be ascribed to the setting-up and growing of the pseudonematic domains inside the isotropic phase. The tumbling motion of a single particle within a pseudonematic domain is moderately density dependent, since the local structure changes smoothly with density even across the INPT. Conversely, the surviving anisotropy relaxes slower and slower on approaching the phase transition.[32]

Within the description provided by eq 11, the dynamics intermediate between the fast and slow monoexponential decays appears to follow a nonexponential relaxation that can be described by a stretched-exponential term, whose exponent ξ approaches the value of unity moving away from the INPT. This is the expected trend obtained on decreasing density. At the same time, it appears that the difference among the three characteristic times tends to become smaller on passing from state point **I** to state point **IV**, and, particularly, fast and intermediate characteristic times, δ and υ, tend to become equal. There may a parallelism between the exponential nature of the fastest dynamics and the nonexponential nature of the intermediate dynamics observed in our numerical data described with eq 11, and the molecular dynamics simulation results reported in ref 39 for a polymer liquid undergoing a glass transition. In the latter work, it was found that the short-time dynamics of the polymer liquid and glass investigated could be separated into two regimes, with the fast one being Debye-like and the slower one following a stretched exponential function. It was argued that, while the first process is related to the motion of polymeric segments within a cage of nearest neighbors, the second involves a cooperative rearrangements of groups of segments. In our case, the fast monoexponential relaxation should mainly account for the local tumbling motion of a particle inside its nearest-neighbor cage, while the stretched exponential term may be connected with the coupling of single-particle relaxation with the relaxation of the pseudonematic domain to

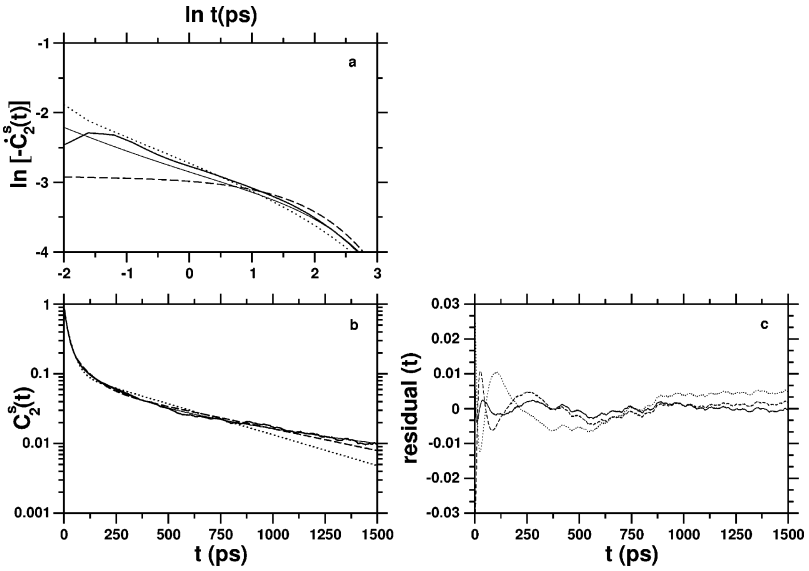

Figure 7. (a) log−log plot of the time derivative of the single-particle orientational correlation functions at short times for state point **I** (bold solid line), compared with the curves obtained via fitting through eq 9 (dotted line), eq 11 (thin solid line), and eq 12 (dashed line). (b) Semilogarithmic plot of the single-particle orientational correlation function for state point **I** (bold solid line), compared with curves obtained via fitting through eq 9 (dotted line), eq 11 (thin solid line), and eq 12 (dashed line). (c) Linear plot of the absolute value of the residual[38] between simulated and fitting values for state point **I**, using as fitting functions eq 9 (dotted line), eq 11 (thin solid line), and eq 12 (dashed line).

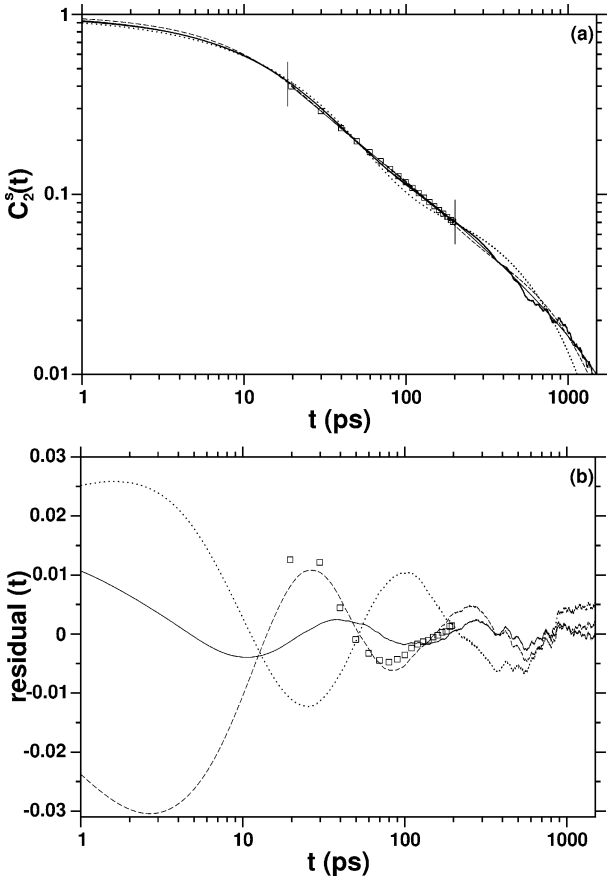

Figure 8. (a) log−log plot of the single-particle orientational correlation function for state point **I** (bold solid line) compared with the curves obtained via fitting through eq 9 (dotted line), eq 11 (thin solid line), and eq 12 (dashed line). The linear fit is represented by squares and is bracketed by the two vertical lines. (b) Plot of the residuals, that is the difference between simulation and fitting results (lines and symbols as in part a).

which it belongs. Similar comments were made in ref 32, although on the basis of a biexponential function. The single-particle functions then have a very small residual anisotropy which relaxes exponentially at longer times and should be intimately related with the LDG relaxation of the pseudonematic domains.

In previous computer simulations performed on the GB model,[18,19] it was found that in the vicinity of the INPT the single-particle orientational correlation functions themselves possess a linear region in their log−log plot. The values of the slope were −0.56 in ref 18, and −0.70 in ref 19. For state point **I** of our spherocylinder-like particle system, we do find that, for an appropriately chosen time window, namely between ∼20 and ∼200 ps, the decay of $C_2^s(t)$ appears reasonably of the power law type, with a value of the above-mentioned slope in the log−log plot of −0.77 (Figure 8). This might indicate a qualitative general behavior in the shape of the single-particle orientational relaxation function in the vicinity of the INPT, that outweigths the differences between the two models, evidenced by the unequal values of the slope, whatever values is selected for the GB model. However, as it is shown in Figure 8, this finding does not prove a power law behavior in the $C_2^s(t)$ itself, as the assumed linear portion of its log−log plot can be explained resorting to the function $S(t)$ (eq 11).

3.2. Collective Orientational Relaxation. The collective orientational correlation functions have been evaluated for the time interval 0−1.5 ns and are affected by an error, estimated according to ref 37, of 20% at most (Figure 9). The rather high

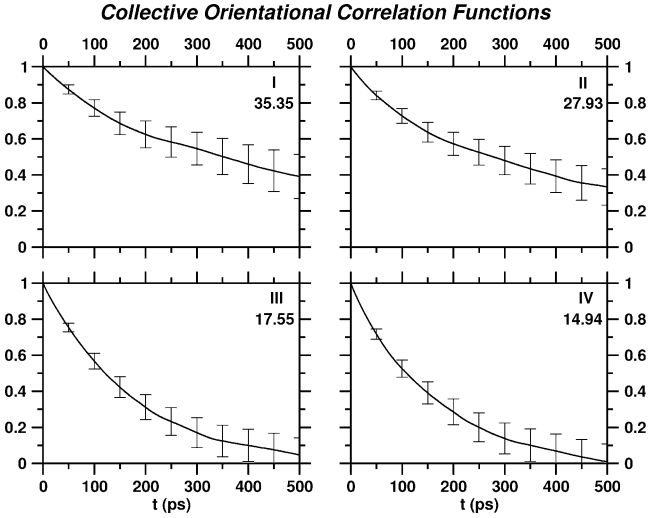

Figure 9. Normalized collective orientational correlation functions obtained in the simulations with their error bars. The number in every panel refers to the value at $t = 0$ of the un-normalized $C_2^c(t)$.

TABLE 2: Parameters of the Fittings of the Functions $C_2^s(t)$ Obtained in Simulations: (a) via Eq 7; (b) via Eq 9; (c) via Eq 11; (d) via Eq 12

	state point	τ_{LDG}(ps)	a	γ (ps)	rms
a	**I**	394.3	0.13	19.3	0.008
	II	307.7	0.10	19.0	0.007
	III	71.8	0.20	17.0	0.003
	IV	37.0	0.17	8.7	0.002

	state point	τ_{LDG}(ps)	α	K (ps)	ϵ	p	λ	rms
b	**I**	488.8	0.02	32.6	0.0	0.35	0.15	0.005
	II	443.7	0.09	29.7	0.0	0.31	0.98	0.003
	III	109.1	0.09	21.4	0.0	0.22	0.69	0.001
	IV	57.8	0.05	10.5	0.0	0.21	0.50	0.0008

	state point	τ_{LDG}(ps)	q_1	v (ps)	ξ	q_2	δ (ps)	rms
c	**I**	1255.4	0.03	42.4	0.51	0.40	16.9	0.001
	II	817.5	0.03	26.9	0.59	0.41	16.7	0.0008
	III	127.9	0.07	17.3	0.81	0.73	14.1	0.001
	IV	64.4	0.07	8.0	0.82	0.72	8.5	0.0008

	state point	τ_{LDG} (ps)	g_1	γ (ps)	g_2	δ (ps)	rms
d	**I**	690.4	0.07	84.4	0.22	13.8	0.003
	II	581.4	0.05	48.9	0.33	11.9	0.002
	III	111.5	0.10	24.5	0.71	4.9	0.001
	IV	57.2	0.08	11.5	0.76	2.1	0.0008

TABLE 3: Parameters of the Fittings of the Functions $C_2^c(t)$ Obtained in the Simulations via Eq 7

state point	τ_{LDG} (ps)	a	γ(ps)	rms
I	750 ± 300	0.85 ± 0.03	99 ± 14	0.010
II	610 ± 225	0.81 ± 0.03	87 ± 16	0.008
III	150 ± 25	1.0	undefined	0.030
IV	130 ± 20	1.0	undefined	0.050

statistical uncertainty of these collective functions prevents us from a definite assessment of the pros and cons of the various functional fitting forms.

We have found that the collective orientational correlation functions, $C_2^c(t)$, are satisfactorily described by a sum of two exponentials at higher density, and by just one exponential at lower density. In Table 3, we give the parameters of the fittings performed with eq 2, with the constaint $a + b = 1$.

On approaching the INPT, the monoexponential function that models the relaxation of collective orientational correlation functions bifurcates in two exponential terms, a manifestation of the onset and progressive growth of the pseudonematic domains. This phenomenon separates the collective orientational

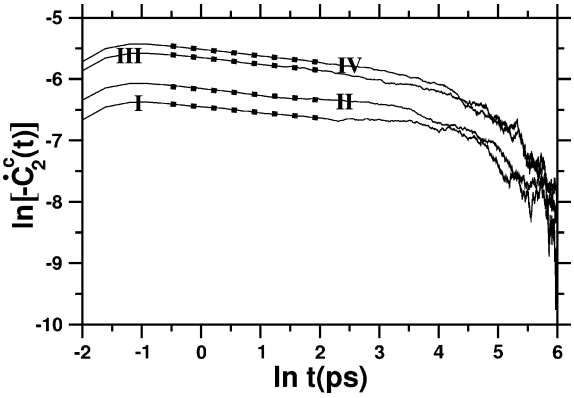

Figure 10. Time derivative of the normalized collective orientational correlation functions on a log−log scale; dotted lines are linear fits with a slope of −0.10.

relaxation into two principal channels, one occurring within a pseudonematic domain and the other involving all the pseudonematic domains of the sample. While intra- and interdomain dynamics are separated in the vicinity of the INPT, they cannot be clearly resolved as we move away enough from the phase transition, where the very idea of pseudonematic domains fades.

In ref 19, the $C_2^c(t)$ functions of the GB model in the vicinity of the INPT have been successfully fitted with a power law, on a time scale short compared to τ_{LDG}. The exponents have been found to be highly density dependent. It appears always feasible to select an appropriate temporal region where a power law provides a good fit to $C_2^c(t)$. However, we believe it not a convincing proof of the existence of a power law decay in the relaxation of the collective orientational correlation functions. Instead, we think it more useful to search for an expression capable of reproducing the numerical data over all the time window examined. In this respect, a biexponential function, eventually merging to one exponential at lower density, seems to produce good results, taking into account the relatively low resolution of the available data. The satisfactory description of the collective orientational correlation functions by a sum of, at most, two exponential terms may in fact be the consequence of their poor statistics (although error bars of $C_2^c(t)$ are not reported in ref 19, they can be assumed of the same magnitude as those in Figure 9). However, it might have a more fundamental origin. The functions $C_2^c(t)$ probe the orientational relaxation of a many-body system, which may be supposed weakly anisotropic. Therefore, they may not show those peculiar features such the power law term that are strongly connected with the anisometry of the body under consideration.

It is reported that the quantities monitored during optical Kerr effect experiments are essentially the time derivatives of the collective orientational correlation functions. We provide these data, $\dot{C}_2^c(t)$, computed at the above-mentioned state points, in Figure 10. We note that, in analogy with what found for the single-particle functions, the $\dot{C}_2^c(t)$ functions behave linearly in a log−log plot, at least in the time window $t \in [0.5;5]$ ps. The value of the slope of the linear fit, ~ -0.1, is essentially independent from the density. The presence of a linear region in the log−log plot of $\dot{C}_2^c(t)$ might indicate that a temporal power law describes the relaxation of these functions at appropriately short times.

On the basis of some experimental evidence,[12−14] the slope of the linear region in the log−log plot, i.e. the exponent of the assumed power law, p, should be linearly related to κ:

$$p = -0.16\kappa + 1.26 \qquad (13)$$

In our case, the slope of the linear region in the log−log plot of $\dot{C}_2^c(t)$ is ~ -0.1, a value close to that, ~ -0.2, estimated from Figure 6 of ref 19, where the same function is plotted for the GB model. Neither our data nor that from ref 19 lays on the straight line, p vs κ, of eq 13. This apparent disagreement with the experimental data may be overcome if we suppose that what is observed in the OKE experiments at very short times is actually a signature of the single-particle dynamics. The values of $-p$ predicted using the empirical straight line deduced from the experiments (eq 13) are -0.46, -0.3 for $\kappa = 5-6$, values that bracket -0.35, the slope of the straight line in Figure 5 of the present work, where $\ln[-\dot{C}_2^s(t)]$ is plotted against $\ln t$. This conjecture is in accord with the discussions about the physical interpretation of an OKE experiments,[9,11,23] and, particularly, with the conclusions drawn in ref 32, where it was stated that, in an OKE experiment, the fast and intermediate relaxations are associated with the single-particle dynamics, while the slow relaxation is a collective phenomenon. The authors of this work arrived at these conclusions by combining OKE experiments on an isotropic liquid crystal with fluorescence experiments on a properly chosen probe solute dissolved in the same isotropic liquid crystal. In ref 32, each of the three relaxation channels were described by an exponential term, while in the present work we have found that a better representation of the temporal decay is achieved if the second term is replaced by a stretched-exponential.

4. Conclusions

We have performed an MD-NVE computer simulation study of a calamitic liquid-crystal model at four state points in the isotropic phase. The model consists of rodlike particles, each formed by nine soft spheres held rigidly on a line, giving a resulting shape similar to that of a spherocylinder of aspect ratio approximately equal to $\simeq 5-6$. The study has focused on the calculation of second-rank single-particle and collective orientational correlation functions on approaching the phase transition to a nematic fluid. The interest in the subject is particularly motivated by the results of recent optical Kerr effect experiments that report a power law decay of the time derivative of the second-rank collective orientational correlation functions at short times. The power law exponent deduced from a fitting of the experimental data was found to be temperature independent in the vicinity of the phase transition and roughly dependent on the length-to-breadth ratio of the nematogenic molecules. Our computer simulation data do not contradict this picture, in that the time derivative of both single-particle and collective functions exhibits, in a log−log plot, a linear region at short times, with a slope essentially independent from the thermodynamic state, if this is sufficiently close to the phase transition. The value of this slope for the time derivative of the single-particle orientational correlation functions is in reasonable accord with the experimentally determined linear dependence of the latter on the molecular aspect ratio, suggesting that OKE experiments probe single-particle dynamics at short times. However, the single-particle functions are better described by a functional form which is the sum of a fast exponential, an intermediate stretched-exponential and a slow exponential. The decay of the collective functions is described by a biexponetial functional form in the vicinity of the IN phase transition, while, moving away from it, the two exponentials "coalesce" in just one.

Our simulation data neither prove nor rule out definitely the existence of a temporal power law in the decay of the time derivative of the orientational correlation functions in the isotropic phase of a liquid crystal. Its signature is found to be weak by both computer simulations and experiments, being the linear region in the log−log plot of the relevant functions present

in a quite short time interval at short times. If this power law term is indeed present, it may be the result of an orientational relaxation described not only by eq 9 but also, and even more accurately, by a stretched-exponential function as in eq 11.

The emergence of a power law in the decay of orientational correlation functions appears indeed a very fine detail and a definite assessment of its presence by computer simulations would necessitate an exceptionally good statistics. To reach it, very large systems must be simulated for very long times, an exercise which requires a huge computer time even for the simplest models possessing both translational and rotational degrees of freedom.

One alternative may be to resort to the LL model, where the translational motion of the particles is frozen, being the latter confined at the sites of a regular simple lattice. This approximation implies a significant reduction of the computational cost, yet it should keep the essential features responsible of the orientational behavior of an isotropic liquid crystal close to the transition to the nematic phase. The single molecular dynamics simulation of the LL model was described in ref 40 many years ago, and it may be extended to calculate single-particle and collective orientational correlation functions.

Natural extensions of the present calculations that are planned for the future include the following: (a) systems of particles of different aspect ratios, that certainly would guarantee a more complete comparison with experiments allowing for a study on how the orientational correlation function shape changes with κ; (b) systems of particles interacting not only through soft repulsions but also via dispersion attractions and electrostatic interactions, to study how these additional features of the pair potential affect the orientational relaxation dynamics.

The decay times found in the present work are, roughly, 1−2 orders of magnitude smaller than the corresponding experimental quantities. This discrepancy, also found for translational dynamic properties, such as diffusion coefficients and viscosities, can be partly explained as a consequence of the very low value of the mass adopted for our particles (this can be seen by transforming real time in reduced time, and the latter back again to real time with a proper value of the particle mass[22]). Features neglected in our model, but typical of real mesogenic molecules, like biaxiality and flexibility, may be crucial in establishing the correct order of magnitude of dynamic quantities. The MD simulations on semiflexible beadlace particles[41] and the atomistic MD simulation on a 5CB model[42] are expected to provide data that might support the hypothesis of a relation between molecular flexibility and nonexponential behavior of the single-particle orientational relaxation at very short times, earlier proposed in an MD study of the PCH5 nematogen.[43]

The elucidation of the short-time dynamics in isotropic liquid crystals may also benefit from detailed computer simulation studies on the orientational relaxation of solutes dissolved in isotropic nematogenic solvents. It would be, in fact, interesting to investigate how the nature of the reorientational motion of the solute changes with its size and shape, keeping the same solvent particles. This project, a fortiori limited to the calculation of single-particle orientational correlation functions, has the advantage of being feasible with a relatively modest computational effort.

Finally, we would like to end up with a comment on possible future experiments. To cast light on the relationships between the power law exponent and the molecular aspect ratio, the experimental techniques might be applied to the members of the para-*n*-phenyls series, with $n \geq 5$, whose value of κ is more confidently defined.

Note Added in Proof

After our paper had been accepted, Chakrabarti et al.[44] reported new results of orientational relaxation from computer simulation on a calamitic, a discotic, and a lattice nematic liquid crystal model. Although these data are considered to support the existence of a universal power law behavior, we make the following remarks: (1) The plots shown in Figure 1 relate to the single-particle orientational time correlations functions and *not* to their time derivatives. (2) A more detailed account of the fitting procedure (which model functions have been used, the corresponding rms errors, etc.) is needed before a thorough comparison with our results can be made as well before definite conclusions can be drawn about the matter. (3) We share the point of view that using a lattice model would be advantagious in that it permits one to simulate a larger system for a longer time. However, in our opinion a much larger increment of the particle number than the 1000 rotors considered would be necessary.

References and Notes

(1) De Gennes, P. G. *The Physics of Liquid Crystals*; Clarendon Press: Oxford 1974.

(2) *Introduction to Liquid Crystals*; Priestley, E. B., Wojtowicz, P. J., Sheng, P., Eds.; Plenum Press: New York, 1975.

(3) Lebwohl, P. A.; Lasher, G. *Phys. Rev. A* **1972**, *6*, 426. Lebwohl, P. A.; Lasher, G. *Phys. Rev. A* **1973**, *7*, 2222.

(4) Chiccoli, C.; Pasini, P.; Zannoni, C. *Advances in the Computer Simulation of Liquid Crystals*; Pasini, P., Zannoni, C., Eds.; Kluwer: Dordrecht 2000; Chapters 6 and 7.

(5) Allen, M. P.; Warren, M. A. *Phys. Rev. Lett.* **1997**, *78*, 1291.

(6) Maier, W.; Saupe, A. *Z. Naturforsch.***1959**, *14a*, 882. Maier, W.; Saupe, A. *Z. Naturforsch.* **1960**, *15a*, 287.

(7) Fabbri, U.; Zannoni, C. *Mol. Phys.* **1986**, *58*, 763.

(8) Zhang, Z.; Mouritsen, O. G.; Zuckermann, M. J. *Phys. Rev. Lett.* **1992**, *69*, 2803.

(9) Deeg, F. W.; Greenfield, S. R.; Stankus, J. J.; Newell, V. J.; Fayer, M. D. *J. Chem. Phys.* **1990**, *93*, 3503.

(10) Stankus, J. J.; Torre, R.; Marshall, C. D.; Greenfield, S. R.; Sengupta, A.; Tokmakoff, A.; Fayer, M. D. *Chem. Phys. Lett.* **1992**, *194*, 213.

(11) Stankus, J. J.; Torre, R.; Fayer, M. D. *J. Phys. Chem.* **1993**, *97*, 9478.

(12) Gottke, S. D.; Brace, D. D.; Cang, H.; Bagchi, B.; Fayer, M. D. *J. Chem. Phys.* **2002**, *116*, 360.

(13) Gottke, S. D.; Cang, H.; Bagchi, B.; Fayer, M. D. *J. Chem. Phys.* **2002**, *116*, 6339.

(14) Cang, H.; Li, J.; Fayer, M. D. *Chem. Phys. Lett.* **2002**, *366*, 82.

(15) Sengupta, A.; Fayer, M. D. *J. Chem. Phys.* **1995**, *102*, 4193.

(16) Allen, M. P.; Frenkel, D. *Phys. Rev. Lett.* **1987**, *58*, 1748.

(17) Perera, A.; Ravichandran, S.; Moreau, M.; Bagchi, B. *J. Chem. Phys.* **1997**, *106*, 1280.

(18) Ravichandran, S.; Perera, A.; Moreau, M.; Bagchi, B. *J. Chem. Phys.* **1998**, *109*, 7349.

(19) Jose, P. P.; Bagchi, B. *J. Chem. Phys.* **2004**, *120*, 11256.

(20) Allen, M. P.; Evans, G. T.; Frenkel, D.; Mulder, B. M. *Adv. Chem. Phys.* **1993**, *86*, 1.

(21) Cinacchi, G.; De Gaetani, L.; Tani, A. *Phys. Rev. E* **2005**, *71*, 031703.

(22) Cinacchi, G.; De Gaetani, L.; Tani, A. *J. Chem. Phys.* **2005**, *122*, 184513.

(23) Cang, H.; Li, J.; Novikov, V. N.; Fayer, M. D. *J. Chem. Phys.* **2003**, *118*, 9303.

(24) Cang, H.; Li, J.; Novikov, V. N.; Fayer, M. D. *J. Chem. Phys.* **2003**, *119*, 10421.

(25) Kohlrausch, R.*Ann. Phys.* **1847**, *12*, 393.

(26) Williams, G.; Watts, D. C. *Trans. Faraday Soc.* **1970**, *66*, 80.

(27) Shlesinger, M. F.; Montroll, E. W. *Proc. Natl. Acad. Sci. U.S.A.* **1984**, *81*, 1280.

(28) Palmer, R. G.; Stein, D. L.; Abrahams, E.; Anderson, P. W. *Phys. Rev. Lett.* **1984**, *53*, 958.

(29) Jose, P. P.; Chakrabati, D.; Bagchi, B. *Phys. Rev. E* **2005**, *71*, 030701(R).

(30) Torre, R.; Ricci, M.; Saielli, G.; Bartolini, P.; Righini, R. *Mol. Cryst. Liq. Cryst.* **1995**, *262*, 391.

(31) Torre, R.; Califano, S. *J. Chim. Phys.* **1996**, *93*, 1843.

(32) Torre, R.; Tempestini, F.; Bartolini, P.; Righini, R. *Philos. Mag. B* **1998**, *77*, 645.

(33) Hyun, B. R.; Quitevis, E. L. *Chem. Phys. Lett.* **2003**, *370*, 725. Hyun, B. R.; Quitevis, E. L. *Chem. Phys. Lett.* **2003**, *373*, 526.

(34) Hunt, N. T.; Meech, S. R. *J. Chem. Phys.* **2004**, *120*, 10828.

(35) Choi, M.; Jin, D.; Kim, H.; Kang, T. J.; Jeoung, S. C.; Kim, D. *J. Phys. Chem. B* **1997**, *101*, 8092.

(36) Dutt, G. B. *J. Chem. Phys.* **2003**, *119*, 11971.

(37) Zwanzig, R.; Ailawadi, N. K. *Phys. Rev.* **1969**, *182*, 280.

(38) The fittings of the single-particle and collective orientational correlation functions as well as of their time derivatives with all the functional forms of the text have been carried out by minimizing the root-mean-square deviation (RMS) defined as:

$$\mathrm{RMS} = \left[\frac{1}{N_t}\sum_{i=1}^{N_t}(y_{sim}(t_{i-1}) - y_{fit}(t_{i-1}))^2\right]^{1/2}$$

The sum runs over the N_t times, t_{i-1}, spaced every 0.1 ps, at which the orientational correlation functions have been evaluated. The symbols y_{sim}- and y_{fit} are self-explanatory.

(39) Roe, R. J. *J. Chem. Phys.* **1994**, *100*, 1610.

(40) Zannoni, C.; Guerra, M. *Mol. Phys.* **1981**, *44*, 849.

(41) Cinacchi, G.; De Gaetani, L.; Tani, A. Work in progress.

(42) De Gaetani, L.; Prampolini, G.; Tani, A. Work in progress.

(43) Yakovenko, S. Y.; Kroemer, G.; Geiger, A. *Mol. Cryst. Liq. Cryst.* **1996**, *275*, 91.

(44) Chakrabarti, D.; Jose, P. P.; Chakrabarty, S.; Bagchi, B. *Phys. Rev. Lett.* **2005**, *95*, 197801.